

Impact of model developments on permafrost simulation in JULES

S. E. Chadburn et al.

Impact of model developments on present and future simulations of permafrost in a global land-surface model

S. E. Chadburn¹, E. J. Burke², R. L. H. Essery³, J. Boike⁴, M. Langer^{4,5},
M. Heikenfeld^{4,6}, P. M. Cox¹, and P. Friedlingstein¹

¹Earth System Sciences, Laver Building, University of Exeter, North Park Road, Exeter EX4 4QE, UK

²Met Office Hadley Centre, Fitzroy Road, Exeter EX1 3PB, UK

³Grant Institute, The King's Buildings, James Hutton Road, Edinburgh EH9 3FE, UK

⁴Alfred Wegener Institute, Helmholtz Center for Polar and Marine Research (AWI) 14473 Potsdam, Germany

⁵Laboratoire de Glaciologie et Géophysique de l'Environnement (LGGE) BP 96 38402 St Martin d'Hères Cedex, France

⁶Atmospheric, Oceanic and Planetary Physics, Department of Physics, University of Oxford, Parks Road, Oxford OX1 3PU, UK

Title Page

Abstract

Introduction

Conclusions

References

Tables

Figures



Back

Close

Full Screen / Esc

Printer-friendly Version

Interactive Discussion



Received: 25 February 2015 – Accepted: 9 March 2015 – Published: 25 March 2015

Correspondence to: S. E. Chadburn (s.e.chadburn@exeter.ac.uk)

Published by Copernicus Publications on behalf of the European Geosciences Union.

TCD

9, 1965–2012, 2015

Impact of model developments on permafrost simulation in JULES

S. E. Chadburn et al.

Title Page

Abstract

Introduction

Conclusions

References

Tables

Figures



Back

Close

Full Screen / Esc

Printer-friendly Version

Interactive Discussion



Abstract

There is a large amount of organic carbon stored in permafrost in the northern high latitudes, which may become vulnerable to microbial decomposition under future climate warming. In order to estimate this potential carbon-climate feedback it is necessary to correctly simulate the physical dynamics of permafrost within global Earth System Models (ESMs) and to determine the rate at which it will thaw.

Additional new processes within JULES, the land surface scheme of the UK ESM (UKESM), include a representation of organic soils, moss and bedrock, and a modification to the snow scheme. The impact of a higher vertical soil resolution and deeper soil column is also considered.

Evaluation against a large group of sites shows the annual cycle of soil temperatures is approximately 25 % too large in the standard JULES version, but this error is corrected by the model improvements, in particular by deeper soil, organic soils, moss and the modified snow scheme. Comparing with active layer monitoring sites shows that the active layer is on average just over 1 m too deep in the standard model version, and this bias is reduced by 70 cm in the improved version. Increasing the soil vertical resolution allows the full range of active layer depths to be simulated, where by contrast with a poorly resolved soil, at least 50 % of the permafrost area has a maximum thaw depth at the centre of the bottom soil layer. Thus all the model modifications are seen to improve the permafrost simulations.

Historical permafrost area corresponds fairly well to observations in all simulations, covering an area between 14–19 million km². Simulations under two future climate scenarios show a reduced sensitivity of permafrost degradation to temperature, with the near-surface permafrost lost per degree of warming reduced from 1.5 million km² °C⁻¹ in the standard version of JULES to between 1.1 and 1.2 million km² °C⁻¹ in the new model version. However, the near-surface permafrost area is still projected to approximately half by the end of the 21st century under the RCP8.5 scenario.

TCD

9, 1965–2012, 2015

Impact of model developments on permafrost simulation in JULES

S. E. Chadburn et al.

Title Page

Abstract

Introduction

Conclusions

References

Tables

Figures

◀

▶

◀

▶

Back

Close

Full Screen / Esc

Printer-friendly Version

Interactive Discussion



Impact of model developments on permafrost simulation in JULES

S. E. Chadburn et al.

Title Page

Abstract

Introduction

Conclusions

References

Tables

Figures

◀

▶

◀

▶

Back

Close

Full Screen / Esc

Printer-friendly Version

Interactive Discussion



ics rather than by the driving climate. Several land-surface schemes have since been modified to better represent processes that are important for permafrost, for example by including soil freezing, soil organic matter, and improving the representation of snow (Beringer et al., 2001; Lawrence and Slater, 2008; Gouttevin et al., 2012a; Ekici et al., 2014a; Paquin and Sushama, 2014).

This paper demonstrates the impact of adding new permafrost-related processes into JULES (Joint UK Land Environment Simulator Best et al., 2011; Clark et al., 2011), the land-surface scheme used in the UK Earth System Model (UKESM). Although the scarcity and uncertainty of global data on permafrost limits the detail with which it can be represented in a large-scale model like JULES, it is possible to capture the broad spatial patterns of permafrost and active layer thickness (ALT), and to realistically simulate present-day conditions. Chadburn et al. (2015) describe in detail the relevant developments within JULES. These include the effects of organic matter, moss, a deeper soil column and a modification to the snow scheme. Chadburn et al. (2015) also show how these developments impact model simulations at a high Arctic tundra site. This paper now applies them to large-scale simulations, showing that they improve the model performance on a large scale, and significantly impact the simulation of permafrost under future climate scenarios. These developments result in a more appropriate representation of the physical state of the permafrost – a necessary precursor to considering the permafrost carbon feedback.

2 Methods

2.1 Standard model description

JULES is the stand-alone version of the land surface scheme in the Hadley Centre climate models (Best et al., 2011; Clark et al., 2011), and was originally based on the Met Office Surface Exchange Scheme (MOSES) (Cox et al., 1999; Essery et al., 2003). It combines a complex energy and water balance model with a dy-

5 namic vegetation model. JULES is a community model and is publically available from <http://www.jchmr.org/jules>. The work discussed here uses a JULES version 3.4.1 augmented with improved physical processes.

10 JULES represents the physical, biophysical and biochemical processes that control the exchange of radiation, heat, water and carbon between the land surface and the atmosphere. It can be applied at a point or over a grid, and requires temporally continuous atmospheric forcing data at frequencies of 3 h or greater. Each grid box can contain several different land-covers or “tiles”, including a number of different plant functional types (PFT’s) as well as non-vegetated tiles (urban, water, ice and bare soil). Each tile has its own surface energy balance, but the soil underneath is treated as a single column and receives aggregated fluxes from the surface tiles.

15 Recently a multi-layer snow scheme has been adopted in JULES (described in Best et al., 2011) in which the number of snow layers varies according to the depth of the snow pack. Each snow layer has a prognostic temperature, density, grain size and solid and liquid water content. This scheme significantly improves simulations of winter soil temperatures in the northern high latitudes (Burke et al., 2013). In the old, zero-layer snow scheme, the insulation from snow was incorporated into the top layer of the soil. This scheme is currently still used when the snow depth is below 10 cm.

20 The subsurface temperatures are modelled via a discretization of both heat diffusion and heat advection by moisture fluxes. The soil thermal characteristics depend on the moisture content, as does the latent heat of freezing and thawing. A zero-heat-flux condition is applied at the lower boundary. The soil hydrology is based on a finite difference approximation to the Richards’ equation (Richards, 1931), using the same vertical discretisation as the soil thermodynamics (Cox et al., 1999). JULES uses the Brooks and Corey (1964) relations to describe the soil water retention curve and calculate hydraulic conductivity and soil water suction. The soil hydraulic parameters are calculated according to Cosby et al. (1984). The default vertical discretisation is a 3 m column modelled as 4 layers, with thicknesses of 0.1, 0.25, 0.65 and 2 m.

Impact of model developments on permafrost simulation in JULES

S. E. Chadburn et al.

Title Page

Abstract

Introduction

Conclusions

References

Tables

Figures



Back

Close

Full Screen / Esc

Printer-friendly Version

Interactive Discussion



Chadburn et al. (2015) allows the multilayer snow scheme to run with arbitrarily thin layers.

2.3 Applying model developments on a global scale

The following sections describe how the spatial distribution of organic matter and moss was determined for a large-scale simulation. The depth of the soil column was fixed across the globe, although there is scope for further improvement to this, for example using a spatially variable depth-to-bedrock as in recent work by Paquin and Sushama (2014).

2.3.1 Global organic matter distribution

The organic fractions were calculated from a combination of the Northern Circumpolar Soil Carbon Database (NCSCD) (Hugelius et al., 2013) where available, and the Harmonized World Soil Database (HWSD) (FAO/IIASA/ISRIC/ISS-CAS/JRC, 2012) for the rest of the land surface. These databases include some rather limited information about the vertical distribution of soil carbon. Using this, an approximate vertical profile of soil carbon was prescribed for each grid cell (see Eq. 1) and the soil properties calculated accordingly for each model level.

Organic carbon quantities can be obtained from both the NCSCD and HWSD datasets for the top 30 cm (C_{30}) and top 1 m (C_{100}). The profile of soil carbon was assumed to be a constant plus an exponential term. The total for the top 1 m adds up to the observed amount.

$$C(z) = \frac{C_{100} - C_{30}}{0.7} + \left(\frac{C_{30}}{0.3} - \frac{C_{100} - C_{30}}{0.7} \right) \exp\left(-\frac{z}{0.3}\right) \quad (1)$$

when $z < 3$ m and $C(z) = 0$ otherwise.

This form of the profile is based on the generic profiles in (Harden et al., 2012) (Fig. 2). It assumes that an exponential distribution of carbon is appropriate and that

Impact of model developments on permafrost simulation in JULES

S. E. Chadburn et al.

Title Page

Abstract

Introduction

Conclusions

References

Tables

Figures

◀

▶

◀

▶

Back

Close

Full Screen / Esc

Printer-friendly Version

Interactive Discussion



there is no carbon below 3 m. In reality some carbon will be found below 3 m, but it is not likely to have a great impact on the soil properties, which are somewhat uncertain anyway for the deeper ground. Figure 1 shows profiles generated using this method for a warm soil grid cell and a high latitude grid cell.

2.3.2 Dynamic moss

There are no datasets showing the pan-Arctic distribution of mosses. In addition in a changing climate the distribution of moss may also change. Therefore, moss was implemented in JULES so that it can be run either with a static map that is input at the start of the run, or with dynamic growth determined by environmental conditions in the model.

In order to determine the presence of moss in any grid cell, the model takes account of the local temperature, moisture, light, snow-cover and, in some cases, wind speed (see Table 1). The moss cover is then determined by a “health” variable, whose value is updated once a day depending on the conditions over the past 24 h. Good conditions add to health and bad conditions subtract from it. It is constrained within bounds resulting in maximum health within a year given optimum growing conditions. The conditions for good and poor growth are given in Table 1. The water suction is taken as the minimum of water suctions in the top soil layer and the atmosphere, the temperature, T_s , is that of the top soil layer, and the light is the radiation at the bottom of the canopy. These values are chosen for being closest to the soil surface where moss is located.

The temperature, moisture and light ranges for good growth are based on the values in Proctor (1982). The light saturation and compensation curves (L_{sat} and L_{comp} respectively) were estimated from Proctor (1982) and are given by

$$L_{\text{sat}} = 19 + \exp(0.161T_s) \quad (2)$$

$$L_{\text{comp}} = 0.1 \exp(-0.57T_s) + 0.4 \exp(0.13T_s), \quad (3)$$

Impact of model developments on permafrost simulation in JULES

S. E. Chadburn et al.

Title Page

Abstract

Introduction

Conclusions

References

Tables

Figures

◀

▶

◀

▶

Back

Close

Full Screen / Esc

Printer-friendly Version

Interactive Discussion



where light compensation is the level at which photosynthesis balances respiration, and light saturation is the level at which photosynthesis is no longer light limited (increasing radiation levels no longer increase the rate of photosynthesis).

The heat and moisture conditions that cause the moss to die off are also taken from Proctor (1982). As well as dying in very hot or dry conditions, moss can suffer badly from wind damage when it is frozen (Longton, 1982). Thus the model includes a third scenario in which moss dies off: when it is cold, windy, and there is no protective snow cover.

Snow protects moss from harsh conditions in winter, but of course it cannot actually grow under deep snow, so a small value is subtracted from the health under deep snow. The same occurs when it is too dark or too cold for photosynthesis to take place. Moss growth has been observed up to 2 weeks before the end of snowmelt (Collins and Callaghan, 1980), so the threshold value for growth under snow was assumed based on snow mass values in JULES two weeks before the end of snowmelt. The magnitude of the values added to and subtracted from the health variable were calibrated at several sites where the moss cover was known.

When the moss health is positive, it is taken to have maximum cover in the grid cell. When the health becomes negative, the percentage cover drops off linearly to zero, and the cover is zero for the lowest quartile of health values. If there is other vegetation present, the fractional cover of moss is capped at 0.7 for those vegetation tiles. This value was pragmatically chosen given that moss can have around 50–100% cover in forests (Beringer et al., 2001). Moss cover is assumed to be zero for the urban or ice fraction of a grid box. The relationship of moss health to moss cover would benefit from further calibration.

Figure 2 shows a moss distribution simulated by JULES in the northern high latitudes, and compares it with data from the Euskirchen et al. (2007) land cover map. In general the most densely moss-covered areas correspond to the tundra land-cover classes, which are shown in bright green. Our scheme gives some general representation of this low vegetation cover, which is otherwise missing in JULES. Moss also grows

Impact of model developments on permafrost simulation in JULES

S. E. Chadburn et al.

Title Page

Abstract

Introduction

Conclusions

References

Tables

Figures



Back

Close

Full Screen / Esc

Printer-friendly Version

Interactive Discussion



For the simulations discussed in this paper, the anomalies were re-gridded to 0.5° resolution and applied to a repeating sequence of 8 years of WFDEI reanalysis data (1998–2005). Using anomalies rather than directly using climate model data makes the climate variability in the future simulations more consistent with the historical data. The main disadvantage is that small-scale features are not captured, since sub-monthly variability comes from the base dataset (Hempel et al., 2013).

2.4.3 CALM Network

The Circumpolar Active Layer Monitoring Network (CALM) (Brown et al., 2000, 2003) is a network of over 100 sites at which on going measurements of the end of season thaw depth (the ALT) are taken. Measurements are available from the early 1990's, when the network was formed. The data are available from <http://www.gwu.edu/~calm/data/north.html>.

2.4.4 Historical soil temperatures

The Russian historical soil temperature dataset is described in Frauenfeld et al. (2004). Soil temperatures were measured at 242 stations, over different time periods starting as early as 1890. The measurements used in this paper were taken at depths of 0.2, 0.4, 0.8, 1.6 and 3.2 m using extraction thermometers, with additional measurements at 0.6, 1.2 and 2.4 m. At some of the sites the natural vegetation cover was removed and at others there is some possibility of site disturbance, however the majority of these measurement sites retained their natural vegetation and snow cover.

International Polar Year Thermal State of Permafrost (IPY-TSP) borehole inventory data was compiled in 2007–2009 from both new and existing boreholes, achieving a wide spatial coverage of soil temperature data (Romanovsky, 2010). Data are available in the most part from 2006–2009 at a daily resolution, with temperatures measured at a variety of depths.

Impact of model developments on permafrost simulation in JULES

S. E. Chadburn et al.

Title Page

Abstract

Introduction

Conclusions

References

Tables

Figures

◀

▶

◀

▶

Back

Close

Full Screen / Esc

Printer-friendly Version

Interactive Discussion



2.4.5 Globsnow

The European Space Agency snow water equivalent (SWE) product, GlobSnow (Takala et al., 2011) covers the years 1978–2010 and is available on an EASE-Grid at 25 km resolution. GlobSnow is produced using a combination of satellite-based microwave radiometer and ground-based weather station data.

2.4.6 Permafrost distribution data

The Circum-Arctic map of permafrost and ground-ice conditions (Brown et al., 1998) gives a historical permafrost distribution, which can be compared with permafrost area in the model. The dataset contains information on the distribution and properties of permafrost and ground ice in the Northern Hemisphere (20 to 90°N), with gridded data available at 12.5, 25 km, and 0.5° resolution. It records continuous, discontinuous, sporadic, and isolated permafrost regions, for which the estimated permafrost area is 90–100, 50–90, 10–50 and < 10% respectively. In this work, an estimate of the observed permafrost area is used to compare with the simulated area. For the maximum we assume that permafrost would be simulated in the whole of the continuous and discontinuous area, plus a fraction of permafrost in the areas of sporadic permafrost and isolated patches – the fractions being 0.05 and 0.3 respectively. For the minimum we assume that no permafrost would be found in the sporadic and isolated regions, and that in the continuous and discontinuous zones only a fractional coverage of permafrost is found, this being 0.95 and 0.7 respectively for the two zones. This gives a maximum area of 17.0 million km² and a minimum of 13.7 million km². It is important to note that there is considerable uncertainty in this data which means that the true value could fall outside of this estimate.

is even clearer in these large-scale results: the active layer in min4I has very little variability and little apparent correlation with the observations (see Fig. 4a).

Most of the new model processes reduce the active layer, bringing it into much better agreement with the observations, as shown on Fig. 3. Simulating a deeper soil column reduces the active layer mean for the CALM sites by 0.12 m (min14I to minD). The insulating effects of organic matter and moss have a greater impact, reducing the ALT by a further 0.58 m (orgmossD). The inclusion of organic matter has the single greatest effect, reducing the mean ALT by 0.44 m. Figure 4d shows that with the inclusion of all of the new model processes, the full range of ALT values are captured and the points fall around the 1-to-1 line. There is still an outlying block of points where the active layer in JULES is greater than 3.5 m and much deeper than the measurements. Many of these sites fall along the course of the Mackenzie river in Northern Canada (where JULES simulates very little permafrost – see Fig. 6). Precipitation gauges are sparse in this region so there may be large uncertainties in hydrology (Weedon et al., 2011), and the observed soil temperatures vary greatly from around -1 to -7°C , as a result of various influences including land-cover and snow (Burn and Kokelj, 2009). This is a subject for future investigation.

The active layer thickness is determined by both the annual cycle of soil temperatures and the thermal offset between the air and the soil. Table 3 compares these dynamics in JULES with observations from the IPY-TSP dataset and cold sites from the Russian soil temperature dataset (see Sects. 2.4.4 and 2.6). The root mean squared error (RMSE) is calculated using the mean value of the metric for each site, so it quantifies the extent to which the variability between the sites is correctly simulated. In this table the most relevant values are the offset and attenuation of the annual cycle between the air and 1 m depth in the soil, since the soil surface is not so well-defined in the observations. In the standard JULES set-up (min4I) the total offset is approximately correct, suggesting that the mean soil temperatures are simulated well. However the annual cycle is nearly 25 % too large at 1 m depth.

Impact of model developments on permafrost simulation in JULES

S. E. Chadburn et al.

Title Page

Abstract

Introduction

Conclusions

References

Tables

Figures

◀

▶

◀

▶

Back

Close

Full Screen / Esc

Printer-friendly Version

Interactive Discussion



tween the ALT in JULES and the percentage cover of permafrost from (Brown et al., 1998) (100 % for continuous, 90 % for discontinuous, 50 % for sporadic and 10 % for isolated patches) is high, ranging between -0.37 and -0.51 .

However, there are still places where continuous permafrost is observed but JULES does not simulate permafrost. Figure 7 shows that in most of these areas, JULES simulates far too much snow, which will mean too much insulation in winter leading to soils that are too warm. This is particularly noticeable in North-east Canada, and two areas in North-west Russia. However, for most of the remaining land surface, JULES slightly underestimates the snow water equivalent (SWE). Hancock et al. (2014) showed that JULES generally underestimates SWE when driven by reanalysis datasets.

In the observations, the edge of the permafrost-affected zone corresponds quite closely with the zero-degree isotherm, although there is a gap in Western Russia (red lines on Fig. 6). In the JULES simulations this relationship is less consistent, suggesting more spatial heterogeneity in the relationship between air and soil temperatures. For example, excessive snow cover such as that seen in North-east Canada on Fig. 7 could contribute to this effect.

It is also possible to consider the vertical distribution of permafrost. Figure 8 shows a breakdown of active layer depths for all permafrost points (a) and all points (b) in the simulations. The first thing that is clear from this plot is that the discretization of the soil column has a very large effect on the simulation of permafrost. A series of kinks corresponding to the model discretization is apparent in all the curves, which for the higher-resolution simulations does not significantly impact the overall shape of the curve, but for the low-resolution soil changes it almost beyond recognition. For about 50 % of the permafrost points in min4I, the active layer depth is between 1.8 and 2.2 m, where 2 m is the centre of the bottom model layer.

Figure 8 shows that the vertical distribution of permafrost is affected by all the model improvements, but the most significant impact is that when organic soils and moss are included. Here, the permafrost is generally found nearer to the surface.

Impact of model developments on permafrost simulation in JULES

S. E. Chadburn et al.

Title Page

Abstract

Introduction

Conclusions

References

Tables

Figures

◀

▶

◀

▶

Back

Close

Full Screen / Esc

Printer-friendly Version

Interactive Discussion



On Fig. 8b the amount of permafrost with active layer less than 3 m in each simulation is apparent from the fraction of points that thaw to less than 3 m (generally about 30 % of points). This shows that some simulations have a shallower active layer (so colder soils) but less permafrost, for example compare min14I with min4I, and orgmossDS with minD. This is related to the vertical profile of soil temperatures. For example, due to the combination of processes, the maximum soil temperature in orgmossDS compared with minD is colder near the surface but warmer in the deeper soil. This is seen in the soil temperature profiles on Fig. 9.

The total near-surface permafrost area in each simulation is more clearly seen by looking at the historical period on Fig. 10. For consistency with the definition of permafrost, these values include any grid cells where the ALT was less than 3 m for the past two years (so for example in the first year that a grid cell is frozen, it is not included in the permafrost area but after the second year it is added to the area, so the area changes from year to year). Comparing the deep-soil simulations, minD, minmossD, orgD and orgmossD, we see that adding insulation from organic soils and moss increases the permafrost area, which is consistent with the cooling effect seen in Table 3. In orgmossDS, the near-surface permafrost area is significantly reduced compared with orgmossD, which was also apparent in Fig. 8b. Finally, in the shallow (3 m) simulations (min4I and min14I), the permafrost area is smaller but this is not really meaningful. This is because the zero-heat-flux boundary condition is not correct at 3 m which leads to “edge effects” close to the soil boundary. This is seen on Fig. 9, where the soil temperatures in the mineral soil simulations (min4I, min14I and minD) are very similar near the top of the soil, but the annual cycle in the shallow simulations (min4I and min14I) does not continue to fall off with depth, resulting in a maximum temperature that is much too high at the base of the soil. This shows that diagnosing permafrost as the area with ALT less than 3 m requires a soil column significantly deeper than 3 m.

A range for the observed permafrost area is also shown on Fig. 10. This is estimated from Brown et al. (1998), using assumptions described in Sect. 2.4.6. According to this, the simulated permafrost area in the mineral soil simulations (min4I, min14I, minD)

Impact of model developments on permafrost simulation in JULES

S. E. Chadburn et al.

Title Page

Abstract

Introduction

Conclusions

References

Tables

Figures

◀

▶

◀

▶

Back

Close

Full Screen / Esc

Printer-friendly Version

Interactive Discussion



Impact of model developments on permafrost simulation in JULES

S. E. Chadburn et al.

Title Page

Abstract

Introduction

Conclusions

References

Tables

Figures

◀

▶

◀

▶

Back

Close

Full Screen / Esc

Printer-friendly Version

Interactive Discussion



In RCP 8.5, much of the near-surface permafrost thaws in both simulations. However, in the improved model version, there is significantly more permafrost remaining at the end of the century, particularly in northern Russia, reflecting the reduced sensitivity to warming. However, the areas where permafrost remains in orgmossDS show a strong active layer deepening, significantly more than 1 m in some areas. This suggests that although less permafrost is lost in this simulation, with a further increase in temperature it could disappear. Note that this refers just to permafrost at depths of up to 3 m – deeper permafrost may remain longer.

4 Conclusions

Large-scale simulations have shown improved physical permafrost dynamics in JULES, thanks to a deeper and better-resolved soil column, including the physical effects of moss and organic soils, and an improvement to the snow scheme. The model developments reduce the simulated summer thaw depth and the amplitude of the annual cycle of soil temperatures, and bring both to more realistic values. The rate of permafrost loss under future climate warming is also reduced, as is the inter-annual variability of the permafrost area.

It is important to simulate a reasonable ALT before beginning to consider permafrost carbon feedback. For this we have shown that the depth and resolution of the soil column, and the effects of organic soils are the most important considerations for the model. JULES is now able to simulate large-scale patterns in ALT, as seen in Fig. 4, where comparing with a wide range of sites the points with deep or shallow ALT are now generally captured in the model.

A well-resolved soil is absolutely essential for simulating active layer dynamics. With a poorly-resolved soil it is not possible to simulate ALT variability: the thaw depth depends strongly on the model layers, Fig. 8, and there is very little spatial variability in ALT (Fig. 6), which is unrealistic (see Fig. 4). The importance of soil resolution has not often been emphasised in the literature.

effects. There is some progress being made towards upscaling small-scale processes (Muster et al., 2012; Langer et al., 2013), and large-scale datasets are improving over time, which is important for simulating realistic carbon fluxes.

In this paper we have analysed the large scale degradation of permafrost under two future climate scenarios. This shows a significant reduction in near-surface permafrost area, with up to 1.5 million km² of permafrost loss per degree of high-latitude warming, although this is reduced to approximately 1.1 million km² in the improved model version, showing the importance of these model developments in assessing future permafrost thaw. The impact of organic matter is particularly large, as this alone reduces the sensitivity by approximately 15 % (Table 4). In RCP4.5, permafrost is only lost from the edges of the permafrost zone by the end of the century, but in RCP8.5 the near-surface permafrost disappears entirely from some large regions, with large areas of permafrost remaining only in northern Canada and some parts of Russia. In areas where near-surface permafrost remains, there is a significant thickening of the active layer, which is relevant for consideration of the permafrost carbon feedback.

Acknowledgements. The authors acknowledge financial support by the European Union Seventh Framework Programme (FP7/2007-2013) project PAGE21, under GA282700. E. Burke was supported by the Joint UK DECC/Defra Met Office Hadley Centre Climate Programme GA01101. M. Langer is also supported by a Post-Doctoral Research Fellowship (A. v. Humboldt Foundation).

References

- Alexeev, V. A., Nicolsky, D. J., Romanovsky, V. E., and Lawrence, D. M.: An evaluation of deep soil configurations in the CLM3 for improved representation of permafrost, *Geophys. Res. Lett.*, 34, L09502, doi:10.1029/2007GL029536, 2007. 1986
- Bekryaev, R. V., Polyakov, I. V., and Alexeev, V. A.: Role of polar amplification in long-term surface air temperature variations and modern arctic warming, *J. Climate*, 23, 3888–3906, doi:10.1175/2010JCLI3297.1, 2010. 1968

Impact of model developments on permafrost simulation in JULES

S. E. Chadburn et al.

Title Page

Abstract

Introduction

Conclusions

References

Tables

Figures



Back

Close

Full Screen / Esc

Printer-friendly Version

Interactive Discussion



Impact of model developments on permafrost simulation in JULES

S. E. Chadburn et al.

Title Page

Abstract

Introduction

Conclusions

References

Tables

Figures

◀

▶

◀

▶

Back

Close

Full Screen / Esc

Printer-friendly Version

Interactive Discussion



- Beringer, J., Lynch, A. H., Chapin, F. S., Mack, M., and Bonan, G. B.: The representation of Arctic soils in the Land Surface Model: the importance of mosses, *J. Climate*, 14, 3324–3335, doi:10.1175/1520-0442(2001)014<3324:TROASI>2.0.CO;2, 2001. 1969, 1971, 1975
- Best, M. J., Pryor, M., Clark, D. B., Rooney, G. G., Essery, R. L. H., Ménard, C. B., Edwards, J. M., Hendry, M. A., Porson, A., Gedney, N., Mercado, L. M., Sitch, S., Blyth, E., Boucher, O., Cox, P. M., Grimmond, C. S. B., and Harding, R. J.: The Joint UK Land Environment Simulator (JULES), model description – Part 1: Energy and water fluxes, *Geosci. Model Dev.*, 4, 677–699, doi:10.5194/gmd-4-677-2011, 2011. 1969, 1970
- Bosilovich, M. G., Chen, J., Robertson, F. R., and Adler, R. F.: Evaluation of global precipitation in reanalyses, *J. Appl. Meteorol. Clim.*, 47, 2279–2299, doi:10.1175/2008JAMC1921.1, 2008. 1989
- Brooks, R. and Corey, A.: Hydraulic Properties of Porous Media, Colorado State University Hydrology Papers, Colorado State University, available at: http://books.google.co.uk/books?id=F_1HOgAACAAJ (last access: 27 January 2015), 1964. 1970
- Brown, J., Ferrians Jr., O. J., Heginbottom, J., and Melnikov, E.: Circum-arctic map of permafrost and ground ice conditions, National Snow and Ice Data Center, available at: http://nsidc.org/data/docs/fgdc/ggd318_map_circumarctic (last access: 27 January 2015), 1998. 1978, 1980, 1983, 1984, 1985, 2007, 2011
- Brown, J., Nelson, F. E., and Hinkel, K. M.: The circumpolar active layer monitoring (CALM) program: research designs and initial results, *Polar Geogr.*, 3, 165–258, 2000. 1977
- Brown, J., Hinkel, K. M., and Nelson, F. E.: Circumpolar Active Layer Monitoring (CALM) Program Network, National Snow and Ice Data Center, Boulder, Colorado USA, 2003. 1977
- Burke, E., Dankers, R., Jones, C., and Wiltshire, A.: A retrospective analysis of pan Arctic permafrost using the JULES land surface model, *Clim. Dynam.*, 41, 1025–1038, doi:10.1007/s00382-012-1648-x, 2013. 1970, 1987
- Burke, E. J., Hartley, I. P., and Jones, C. D.: Uncertainties in the global temperature change caused by carbon release from permafrost thawing, *The Cryosphere*, 6, 1063–1076, doi:10.5194/tc-6-1063-2012, 2012. 1968
- Burn, C. R. and Kokelj, S. V.: The environment and permafrost of the Mackenzie Delta area, *Permafrost Periglac.*, 20, 83–105, doi:10.1002/ppp.655, 2009. 1981
- Camill, P.: Permafrost thaw accelerates in boreal peatlands during late-20th century climate warming, *Climatic Change*, 68, 135–152, doi:10.1007/s10584-005-4785-y, 2005. 1968

Impact of model developments on permafrost simulation in JULES

S. E. Chadburn et al.

Title Page

Abstract

Introduction

Conclusions

References

Tables

Figures



Back

Close

Full Screen / Esc

Printer-friendly Version

Interactive Discussion



Chadburn, S., Burke, E., Essery, R., Boike, J., Langer, M., Heikenfeld, M., Cox, P., and Friedlingstein, P.: An improved representation of physical permafrost dynamics in the JULES land surface model, *Geosci. Model Dev. Discuss.*, 8, 715–759, doi:10.5194/gmdd-8-715-2015, 2015. 1969, 1971, 1973, 1979, 1980, 1982

5 Clark, D. B., Mercado, L. M., Sitch, S., Jones, C. D., Gedney, N., Best, M. J., Pryor, M., Rooney, G. G., Essery, R. L. H., Blyth, E., Boucher, O., Harding, R. J., Huntingford, C., and Cox, P. M.: The Joint UK Land Environment Simulator (JULES), model description – Part 2: Carbon fluxes and vegetation dynamics, *Geosci. Model Dev.*, 4, 701–722, doi:10.5194/gmd-4-701-2011, 2011. 1969

10 Collins, N. J. and Callaghan, T. V.: Predicted patterns of photosynthetic production in maritime Antarctic mosses, *Ann. Bot.-London*, 45, 601–620, 1980. 1975

Collins, W., Bellouin, N., Doutriaux-Boucher, M., Gedney, N., Hinton, T., Jones, C. D., Lid-dicoat, S., Martin, G., O'Connor, F., Rae, J., Senior, C., Totterdell, I., Woodward, S., Reichler, T., and Kim, J.: Evaluation of the HadGEM2 model, Met Office Hadley Centre Technical Note no. HCTN 74, Met Office, FitzRoy Road, Exeter EX1 3PB UK, available at: <http://www.metoffice.gov.uk/archive/science/climate-science/hctn74> (last access: 27 January 2015), 2008. 1979

Comiso, J. C.: Large decadal decline of the Arctic multiyear ice cover, *J. Climate*, 25, 1176–1193, doi:10.1175/JCLI-D-11-00113.1, 2012. 1968

20 Cosby, B. J., Hornberger, G. M., Clapp, R. B., and Ginn, T. R.: A statistical exploration of the relationships of soil moisture characteristics to the physical properties of soils, *Water Resour. Res.*, 20, 682–690, doi:10.1029/WR020i006p00682, 1984. 1970

Cox, P. M., Betts, R. A., Bunton, C. B., Essery, R. L. H., Rowntree, P. R., and Smith, J.: The impact of new land surface physics on the GCM simulation of climate and climate sensitivity, *Clim. Dynam.*, 15, 183–203, doi:10.1007/s003820050276, 1999. 1969, 1970

25 Dankers, R., Burke, E. J., and Price, J.: Simulation of permafrost and seasonal thaw depth in the JULES land surface scheme, *The Cryosphere*, 5, 773–790, doi:10.5194/tc-5-773-2011, 2011. 1971, 1972

Dharssi, I., Vidale, P., Verhoef, A., Macpherson, B., Jones, C., and Best, M.: New soil physical properties implemented in the Unified Model at PS18. Meteorology Research and Development technical report 528, Met Office, UK, available at: <http://www.metoffice.gov.uk/archive/forecasting-research-technical-report-528> (last access: 20 March 2015), 2009. 1972

Impact of model developments on permafrost simulation in JULES

S. E. Chadburn et al.

Title Page

Abstract

Introduction

Conclusions

References

Tables

Figures

◀

▶

◀

▶

Back

Close

Full Screen / Esc

Printer-friendly Version

Interactive Discussion



ECMWF (European Center for Medium-Range Weather Forecasts) ECMWF ERA-40 Re-Analysis data, NCAS British Atmospheric Data Centre, available at: http://badc.nerc.ac.uk/view/badc.nerc.ac.uk_ATOM_dataent_12458543158227759 (last access: 27 January 2015), 2009. 1976

5 Ekici, A., Beer, C., Hagemann, S., Boike, J., Langer, M., and Hauck, C.: Simulating high-latitude permafrost regions by the JSBACH terrestrial ecosystem model, *Geosci. Model Dev.*, 7, 631–647, doi:10.5194/gmd-7-631-2014, 2014a. 1969, 1989

Ekici, A., Chadburn, S., Chaudhary, N., Hajdu, L. H., Marmy, A., Peng, S., Boike, J., Burke, E., Friend, A. D., Hauck, C., Krinner, G., Langer, M., Miller, P. A., and Beer, C.: Site-level model
10 intercomparison of high latitude and high altitude soil thermal dynamics in tundra and barren landscapes, *The Cryosphere Discuss.*, 8, 4959–5013, doi:10.5194/tcd-8-4959-2014, 2014b. 1989

Essery, R., Best, M., Betts, R., and Taylor, C.: Explicit representation of subgrid heterogeneity in a GCM land surface scheme, *J. Hydrometeorol.*, 4, 530–543, 2003. 1969

15 Euskirchen, E. S., McGuire, A. D., and Chapin, F. S.: Energy feedbacks of northern high-latitude ecosystems to the climate system due to reduced snow cover during 20th century warming, *Glob. Change Biol.*, 13, 2425–2438, doi:10.1111/j.1365-2486.2007.01450.x, 2007. 1975, 2003

20 FAO/IIASA/ISRIC/ISS-CAS/JRC: Harmonized World Soil Database (version 1.2), FAO, Rome, Italy and IIASA, Laxenburg, Austria, available at: <http://webarchive.iiasa.ac.at/Research/LUC/External-World-soil-database/HTML/> (last access: 20 January 2015), 2012. 1973

Frauenfeld, O. W., Zhang, T., Barry, R. G., and Gilichinsky, D.: Interdecadal changes in seasonal freeze and thaw depths in Russia, *J. Geophys. Res.-Atmos.*, 109, D05101, doi:10.1029/2003JD004245, 2004. 1977

25 Gedney, N. and Cox, P. M.: The sensitivity of global climate model simulations to the representation of soil moisture, *J. Hydrometeorol.*, 4, 1265–1275, doi:10.1175/1525-7541(2003)004<1265:TSGCM>2.0.CO;2, 2003. 1971

Gouttevin, I., Krinner, G., Ciais, P., Polcher, J., and Legout, C.: Multi-scale validation of a new soil freezing scheme for a land-surface model with physically-based hydrology, *The Cryosphere*, 6, 407–430, doi:10.5194/tc-6-407-2012, 2012a. 1969, 1989

30 Gouttevin, I., Menegoz, M., Dominé, F., Krinner, G., Koven, C., Ciais, P., Tarnocai, C., and Boike, J.: How the insulating properties of snow affect soil carbon distribution in the continen-

Impact of model developments on permafrost simulation in JULES

S. E. Chadburn et al.

Title Page

Abstract

Introduction

Conclusions

References

Tables

Figures

◀

▶

◀

▶

Back

Close

Full Screen / Esc

Printer-friendly Version

Interactive Discussion



tal pan-Arctic area, *J. Geophys. Res.-Biogeo.*, 117, G02020, doi:10.1029/2011JG001916, 2012b. 1968

Hancock, S., Huntley, B., Ellis, R., and Baxter, R.: Biases in reanalysis snowfall found by comparing the JULES land surface model to GlobSnow, *J. Climate*, 27, 624–632, doi:10.1175/JCLI-D-13-00382.1, 2014. 1984, 1989

Harden, J. W., Koven, C. D., Ping, C.-L., Hugelius, G., David McGuire, A., Camill, P., Jorgenson, T., Kuhry, P., Michaelson, G. J., O'Donnell, J. A., Schuur, E. A. G., Tarnocai, C., Johnson, K., and Grosse, G.: Field information links permafrost carbon to physical vulnerabilities of thawing, *Geophys. Res. Lett.*, 39, L15704, doi:10.1029/2012GL051958, 2012. 1973

Hempel, S., Frieler, K., Warszawski, L., Schewe, J., and Piontek, F.: A trend-preserving bias correction – the ISI-MIP approach, *Earth Syst. Dynam.*, 4, 219–236, doi:10.5194/esd-4-219-2013, 2013. 1977

Hugelius, G., Tarnocai, C., Broll, G., Canadell, J. G., Kuhry, P., and Swanson, D. K.: The Northern Circumpolar Soil Carbon Database: spatially distributed datasets of soil coverage and soil carbon storage in the northern permafrost regions, *Earth Syst. Sci. Data*, 5, 3–13, doi:10.5194/essd-5-3-2013, 2013. 1973

Hugelius, G., Strauss, J., Zubrzycki, S., Harden, J. W., Schuur, E. A. G., Ping, C.-L., Schirmer, L., Grosse, G., Michaelson, G. J., Koven, C. D., O'Donnell, J. A., Elberling, B., Mishra, U., Camill, P., Yu, Z., Palmtag, J., and Kuhry, P.: Estimated stocks of circumpolar permafrost carbon with quantified uncertainty ranges and identified data gaps, *Biogeosciences*, 11, 6573–6593, doi:10.5194/bg-11-6573-2014, 2014. 1968

Kattsov, V. M., Walsh, J. E., Chapman, W. L., Govorkova, V. A., Pavlova, T. V., and Zhang, X.: Simulation and projection of Arctic freshwater budget components by the IPCC AR4 global climate models, *J. Hydrometeorol.*, 8, 571–589, doi:10.1175/JHM575.1, 2007. 1989

Koven, C., Friedlingstein, P., Ciais, P., Khvorostyanov, D., Krinner, G., and Tarnocai, C.: On the formation of high-latitude soil carbon stocks: effects of cryoturbation and insulation by organic matter in a land surface model, *Geophys. Res. Lett.*, 36, L21501, doi:10.1029/2009GL040150, 2009. 1983

Koven, C. D., Ringeval, B., Friedlingstein, P., Ciais, P., Cadule, P., Khvorostyanov, D., Krinner, G., and Tarnocai, C.: Permafrost carbon–climate feedbacks accelerate global warming, *P. Natl. Acad. Sci. USA*, 108, 14769–14774, doi:10.1073/pnas.1103910108, 2011. 1968

Impact of model developments on permafrost simulation in JULES

S. E. Chadburn et al.

Title Page

Abstract

Introduction

Conclusions

References

Tables

Figures

◀

▶

◀

▶

Back

Close

Full Screen / Esc

Printer-friendly Version

Interactive Discussion



- Koven, C. D., Riley, W. J., and Stern, A.: Analysis of permafrost thermal dynamics and response to climate change in the CMIP5 Earth System Models, *J. Climate*, 26, 1877–1900, doi:10.1175/JCLI-D-12-00228.1, 2012. 1968, 1980, 1987, 2000, 2001
- Langer, M., Westermann, S., Heikenfeld, M., Dorn, W., and Boike, J.: Satellite-based modeling of permafrost temperatures in a tundra lowland landscape, *Remote Sens. Environ.*, 135, 12–24, doi:10.1016/j.rse.2013.03.011, 2013. 1983, 1989, 1990
- Lawrence, D. and Slater, A.: Incorporating organic soil into a global climate model, *Clim. Dynam.*, 30, 145–160, doi:10.1007/s00382-007-0278-1, 2008. 1969, 1989
- Lawrence, D., Slater, A., Romanovsky, V., and Nicolsky, D.: Sensitivity of a model projection of near-surface permafrost degradation to soil column depth and representation of soil organic matter, *J. Geophys. Res.*, 113, F02011, doi:10.1029/2007JF000883, 2008. 1971, 1983, 1986
- Longton, R. E.: Bryophyte vegetation in polar regions, in: *Bryophyte Ecology*, edited by: Smith, A., Springer, London, Chapman and Hall, 123–165, 1982. 1975
- MacDougall, A. H., Avis, C. A., and Weaver, A. J.: Significant contribution to climate warming from the permafrost carbon feedback, *Nat. Geosci.*, 5, 719–721, doi:10.1038/ngeo1573, 2012. 1968
- Mitchell, T. D. and Jones, P. D.: An improved method of constructing a database of monthly climate observations and associated high-resolution grids, *Int. J. Climatol.*, 25, 693–712, doi:10.1002/joc.1181, 2005. 1976
- Muster, S., Langer, M., Heim, B., Westermann, S., and Boike, J.: Subpixel heterogeneity of ice-wedge polygonal tundra: a multi-scale analysis of land cover and evapotranspiration in the Lena River Delta, Siberia, *Tellus B*, 64, 17301, doi:10.3402/tellusb.v64i0.17301, 2012. 1990
- Paquin, J.-P. and Sushama, L.: On the Arctic near-surface permafrost and climate sensitivities to soil and snow model formulations in climate models, *Clim. Dynam.*, 44, 203–228, doi:10.1007/s00382-014-2185-6, 2014. 1969, 1971, 1973
- Proctor, M. C. F.: Physiological ecology: water relations, light and temperature responses, carbon balance, in: *Bryophyte Ecology*, edited by: Smith, A., Springer, London, Chapman and Hall, 333–382, 1982. 1974, 1975
- Richards, L. A.: Capillary conduction of liquids through porous mediums, *J. Appl. Phys.*, 1, 318–333, 1931. 1970
- Rinke, A., Kuhry, P., and Dethloff, K.: Importance of a soil organic layer for Arctic climate: a sensitivity study with an Arctic RCM, *Geophys. Res. Lett.*, 35, L13709, doi:10.1029/2008GL034052, 2008. 1983

Impact of model developments on permafrost simulation in JULES

S. E. Chadburn et al.

Title Page

Abstract Introduction

Conclusions References

Tables Figures

◀ ▶

◀ ▶

Back Close

Full Screen / Esc

Printer-friendly Version

Interactive Discussion



Romanovsky, V. E.: Development of a network of permafrost observatories in North America and Russia: the US contribution to the international polar year., Advanced Cooperative Arctic Data and Information Service, Boulder, CO, available at: https://www.aoncadis.org/project/development_of_a_network_of_permafrost_observatories_in_north_america_and_russia_the_us (last access: 20 March 2015), 2010. 1977

Romanovsky, V. E., Drozdov, D. S., Oberman, N. G., Malkova, G. V., Kholodov, A. L., Marchenko, S. S., Moskalenko, N. G., Sergeev, D. O., Ukraintseva, N. G., Abramov, A. A., Gilichinsky, D. A., and Vasiliev, A. A.: Thermal state of permafrost in Russia, *Permafrost Periglac.*, 21, 136–155, doi:10.1002/ppp.683, 2010. 1968

Schneider von Deimling, T., Meinshausen, M., Levermann, A., Huber, V., Frieler, K., Lawrence, D. M., and Brovkin, V.: Estimating the near-surface permafrost-carbon feedback on global warming, *Biogeosciences*, 9, 649–665, doi:10.5194/bg-9-649-2012, 2012. 1968

Schneider von Deimling, T., Grosse, G., Strauss, J., Schirrmeyer, L., Morgenstern, A., Schaphoff, S., Meinshausen, M., and Boike, J.: Observation-based modelling of permafrost carbon fluxes with accounting for deep carbon deposits and thermokarst activity, *Biogeosciences Discuss.*, 11, 16599–16643, doi:10.5194/bgd-11-16599-2014, 2014. 1968

Schuur, E. A. G., Vogel, J. G., Crummer, K. G., Lee, H., Sickman, J. O., and Osterkamp, T. E.: The effect of permafrost thaw on old carbon release and net carbon exchange from tundra, *Nature*, 459, 556–559, doi:10.1038/nature08031, 2009. 1968

Slater, A. G. and Lawrence, D. M.: Diagnosing present and future permafrost from climate models, *J. Climate*, 26, 5608–8755, doi:10.1175/JCLI-D-12-00341.1, 2013. 1987, 2001

Soudzilovskaia, N. A., van Bodegom, P. M., and Cornelissen, J. H.: Dominant bryophyte control over high-latitude soil temperature fluctuations predicted by heat transfer traits, field moisture regime and laws of thermal insulation, *Funct. Ecol.*, 27, 1442–1454, doi:10.1111/1365-2435.12127, 2013. 1972

Stevens, M. B., Smerdon, J. E., González-Rouco, J. F., Stieglitz, M., and Beltrami, H.: Effects of bottom boundary placement on subsurface heat storage: implications for climate model simulations, *Geophys. Res. Lett.*, 34, L02702, doi:10.1029/2006GL028546, 2007. 1986

Stocker, T., Qin, D., Plattner, G.-K., Tignor, M., Allen, S., Boschung, J., Nauels, A., Xia, Y., Bex, V., and Midgley, P. M. (Eds.): *Climate Change 2013: The Physical Science Basis. Contribution of Working Group I to the Fifth Assessment Report of the Intergovernmental Panel on Climate Change*, IPCC, Cambridge University Press, available at: <http://www.climatechange2013.org/> (last access: 27 January 2015), 2013. 1968

Impact of model developments on permafrost simulation in JULES

S. E. Chadburn et al.

Title Page

Abstract

Introduction

Conclusions

References

Tables

Figures

◀

▶

◀

▶

Back

Close

Full Screen / Esc

Printer-friendly Version

Interactive Discussion



Stroeve, J., Serreze, M., Holland, M., Kay, J., Malanik, J., and Barrett, A.: The Arctic's rapidly shrinking sea ice cover: a research synthesis, *Climatic Change*, 110, 1005–1027, doi:10.1007/s10584-011-0101-1, 2012. 1968

5 Takala, M., Luojus, K., Pulliainen, J., Derksen, C., Lemmetyinen, J., Kärnä, J.-P., Koskinen, J., and Bojkov, B.: Estimating northern hemisphere snow water equivalent for climate research through assimilation of space-borne radiometer data and ground-based measurements, *Remote Sens. Environ.*, 115, 3517–3529, doi:10.1016/j.rse.2011.08.014, 2011. 1978

Weedon, G. P.: Readme file for the “WFDEI” dataset, available at: http://www.eu-watch.org/gfx_content/documents/README-WFDEI.pdf (last access: 27 January 2015), 2013. 1976

10 Weedon, G. P., Gomes, S., Viterbo, P., Österle, H., Adam, J. C., Bellouin, N., Boucher, O., and Best., M.: The WATCH forcing data 1958–2001: a meteorological forcing dataset for land surface- and hydrological-models, WATCH technical report, p. 41, available at: <http://www.eu-watch.org/publications> (last access: 27 January 2015), 2010. 1976

15 Weedon, G. P., Gomes, S., Viterbo, P., Shuttleworth, W. J., Blyth, E., Österle, H., Adam, J. C., Bellouin, N., Boucher, O., and Best, M.: Creation of the WATCH forcing data and its use to assess global and regional reference crop evaporation over land during the twentieth century, *J. Hydrometeorol.*, 12, 823–847, doi:10.1175/2011JHM1369.1, 2011. 1976, 1981

Westermann, S., Schuler, T. V., Gislås, K., and Etzelmüller, B.: Transient thermal modeling of permafrost conditions in Southern Norway, *The Cryosphere*, 7, 719–739, doi:10.5194/tc-7-719-2013, 2013. 1989

20 WGMS: Global Glacier Changes: Facts and Figures, edited by: Zemp, M., Roer, I., Käab, A., Hoelzle, M., Paul, F., Haeberli, W. G., UNEP and World Glacier Monitoring Service, Zurich, Switzerland, 88 pp., 2008. 1968

Impact of model developments on permafrost simulation in JULES

S. E. Chadburn et al.

[Title Page](#)[Abstract](#)[Introduction](#)[Conclusions](#)[References](#)[Tables](#)[Figures](#)[⏪](#)[⏩](#)[◀](#)[▶](#)[Back](#)[Close](#)[Full Screen / Esc](#)[Printer-friendly Version](#)[Interactive Discussion](#)**Table 1.** Conditions for moss growth and die-back.

Health	Water suction	Temperature	Light	Snow mass	Wind speed
+3	< 200 m	$0 < T_s < 27.5^\circ\text{C}$	$> L_{\text{sat}}$	$< 5 \text{ kg m}^{-2}$	–
–3	> 1000 m	–	–	–	–
–3	–	$> 35^\circ\text{C}$	–	–	–
–3	–	$< -5^\circ\text{C}$	–	$< 0.1 \text{ kg m}^{-2}$	$> 12 \text{ ms}^{-1}$
–1	< 1000 m	$< 35^\circ\text{C}$	–	$> 40 \text{ kg m}^{-2}$	–
–1	< 1000 m	$< 35^\circ\text{C}$	$< L_{\text{comp}}$	–*	–*
–1	< 1000 m	$< -5^\circ\text{C}$	–	–*	–*
+1	None of the above.				

* Must not simultaneously satisfy snow mass $< 0.1 \text{ kg m}^{-2}$, wind speed $> 12 \text{ ms}^{-1}$ and temperature $< -5^\circ\text{C}$. For light saturation and compensation curves (L_{sat} and L_{comp}) see Eqs. (2) and (3).

Impact of model developments on permafrost simulation in JULES

S. E. Chadburn et al.

Table 2. List of JULES simulations carried out.

Simulation	Soil layers	Soil depth	Bedrock	Moss	Organic soils	Modified snow
min4l	4	3 m	N	N	N	N
min14l	14	3 m	N	N	N	N
minD	28	10 m	50 m	N	N	N
minmossD	28	10 m	50 m	Y	N	N
orgD	28	10 m	50 m	N	Y	N
orgmossD	28	10 m	50 m	Y	Y	N
orgmossDS	28	10 m	50 m	Y	Y	Y

Title Page

Abstract

Introduction

Conclusions

References

Tables

Figures

◀

▶

◀

▶

Back

Close

Full Screen / Esc

Printer-friendly Version

Interactive Discussion



Impact of model developments on permafrost simulation in JULES

S. E. Chadburn et al.

Table 3. The attenuation of the annual cycle and the thermal offset in the JULES simulations, between the air and the top of the soil, and the top of the soil and 1 m depth, calculated as in (Koven et al., 2012). This includes IPY-TSP data and Russian data for cold sites. The RMSE (root mean squared error) values are based on the mean value of the metric at each site, so give an indication of how well the variability between sites is captured.

Simulation	Attenuation (fraction of amplitude)				Offset (°C)			
	air–0 m	0–1 m	Total	RMSE	air–0 m	0–1 m	Total	RMSE
Observations	0.62	0.40	0.25	–	7.7	–0.25	7.4	–
min4l	0.62	0.50	0.31	0.18	8.5	–1.00	7.5	2.5
min14l	0.67	0.52	0.35	0.20	7.3	–0.57	6.8	2.3
minD	0.68	0.48	0.33	0.20	7.4	–0.72	6.7	2.2
minmossD	0.66	0.48	0.32	0.18	7.2	–0.68	6.5	2.2
orgD	0.65	0.45	0.29	0.17	6.9	–0.92	6.0	2.4
orgmossD	0.62	0.45	0.28	0.16	6.7	–0.87	5.8	2.5
orgmossDS	0.54	0.47	0.25	0.15	8.1	–0.87	7.3	2.4

[Title Page](#)
[Abstract](#)
[Introduction](#)
[Conclusions](#)
[References](#)
[Tables](#)
[Figures](#)
[Back](#)
[Close](#)
[Full Screen / Esc](#)
[Printer-friendly Version](#)
[Interactive Discussion](#)


Impact of model developments on permafrost simulation in JULES

S. E. Chadburn et al.

Title Page

Abstract

Introduction

Conclusions

References

Tables

Figures

◀

▶

◀

▶

Back

Close

Full Screen / Esc

Printer-friendly Version

Interactive Discussion



Table 4. Rate of loss of near-surface permafrost per degree of high-latitude warming in future JULES simulations. The temperature change is calculated over the historical permafrost area (observed).

Simulation	Historical area (10^6 km 2)	Rate of loss (10^6 km 2 °C $^{-1}$)		Rate of loss (fraction °C $^{-1}$)	
		RCP 4.5	RCP 8.5	RCP 4.5	RCP 8.5
min4l	15.5	−1.52	−1.47	0.101	0.097
min14l	14.3	−1.36	−1.32	0.106	0.101
minD	17.0	−1.34	−1.37	0.085	0.087
minmossD	17.7	−1.33	−1.34	0.080	0.080
orgD	18.0	−1.17	−1.21	0.069	0.071
orgmossD	18.7	−1.08	−1.19	0.060	0.066
orgmossDS	16.1	−1.15	−1.11	0.077	0.074
HadGEM2-ES	22–23 ^a	−1.5 ^a	−1.46 ^b	0.065 ^a	

^a Koven et al. (2012), ^b Slater and Lawrence (2013).

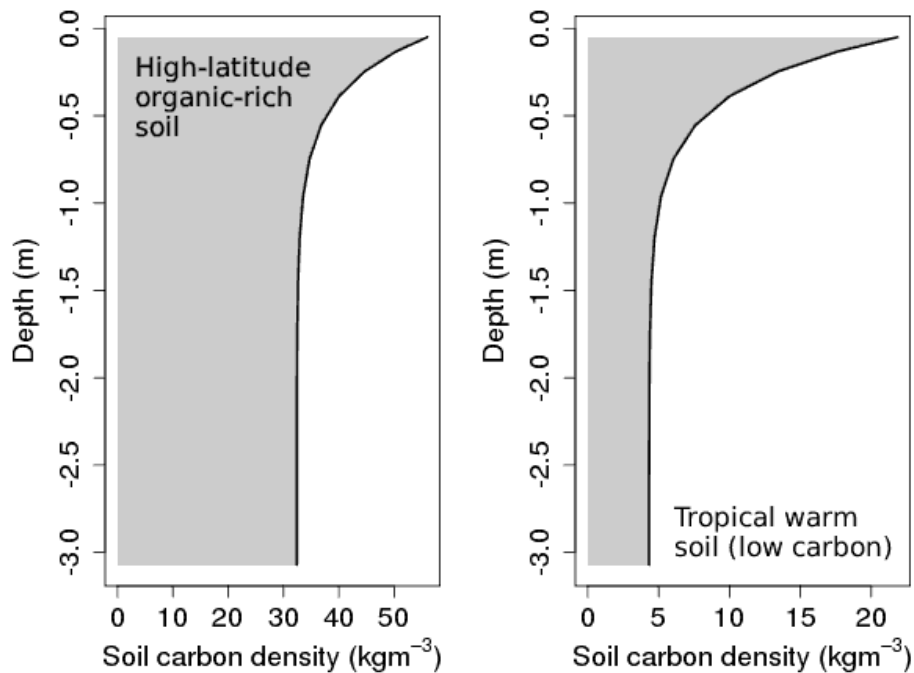


Figure 1. Soil carbon profiles generated using Eq. (1). Left: 119.75° E, 72.25° N, a grid cell with high soil carbon (Siberia). Right: -70.25° E, 4.25° N, a warm location with most of the carbon near the surface (South America).

Impact of model developments on permafrost simulation in JULES

S. E. Chadburn et al.

Title Page	
Abstract	Introduction
Conclusions	References
Tables	Figures
◀	▶
◀	▶
Back	Close
Full Screen / Esc	
Printer-friendly Version	
Interactive Discussion	



Impact of model developments on permafrost simulation in JULES

S. E. Chadburn et al.

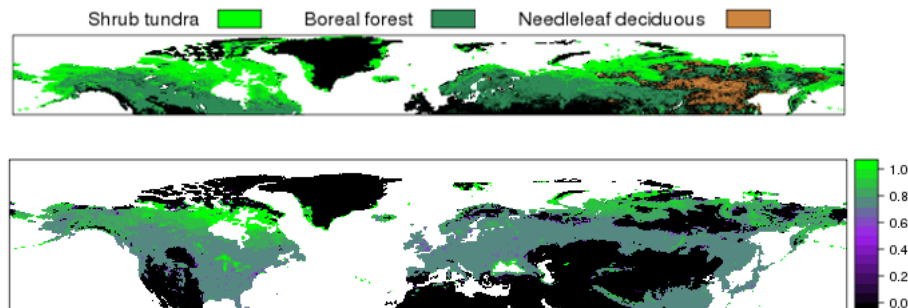


Figure 2. Upper plot: Land cover map using data from Euskirchen et al. (2007). “Shrub tundra” includes prostrate, dwarf shrub and low shrub tundra, and “boreal forest” includes boreal evergreen needleleaf and boreal broadleaf deciduous. Lower plot: Mean moss cover simulated in JULES for the year 2000, from orgmoSSD historical simulation (see Table 2).

[Title Page](#)[Abstract](#)[Introduction](#)[Conclusions](#)[References](#)[Tables](#)[Figures](#)[◀](#)[▶](#)[◀](#)[▶](#)[Back](#)[Close](#)[Full Screen / Esc](#)[Printer-friendly Version](#)[Interactive Discussion](#)

Impact of model developments on permafrost simulation in JULES

S. E. Chadburn et al.

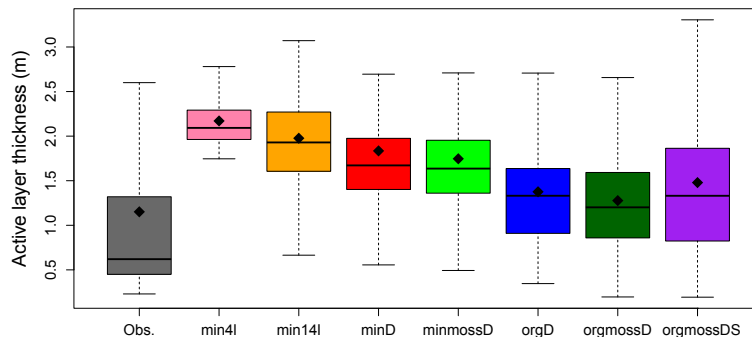


Figure 3. Simulated and observed range of active layer depths for CALM sites (Sect. 2.4.3). Black dots are means, the boxes shows the inter-quartile range (IQR), and the horizontal line is the median. The whiskers indicate the most extreme data point that is no more than 1.5 times the IQR. Outliers are not shown. Points at which either the simulated or observed active layer was very large (greater than 6 m) were removed. The model point for each CALM site is the grid box containing that site.

[Title Page](#)
[Abstract](#)
[Introduction](#)
[Conclusions](#)
[References](#)
[Tables](#)
[Figures](#)
[◀](#)
[▶](#)
[◀](#)
[▶](#)
[Back](#)
[Close](#)
[Full Screen / Esc](#)
[Printer-friendly Version](#)
[Interactive Discussion](#)

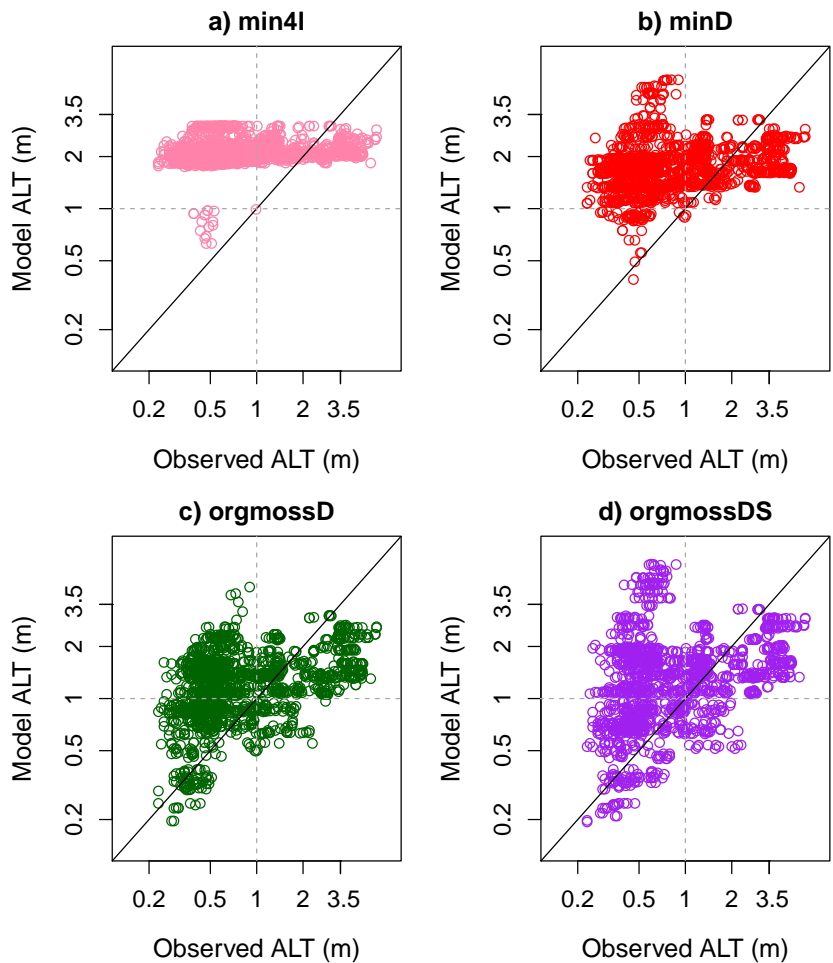



Figure 4. Active layer model values plotted against measurements from CALM dataset (as in Fig. 3). The dashed lines show an ALT of 1 m. Logarithmic axes are used.

Title Page	
Abstract	Introduction
Conclusions	References
Tables	Figures
◀	▶
◀	▶
Back	Close
Full Screen / Esc	
Printer-friendly Version	
Interactive Discussion	



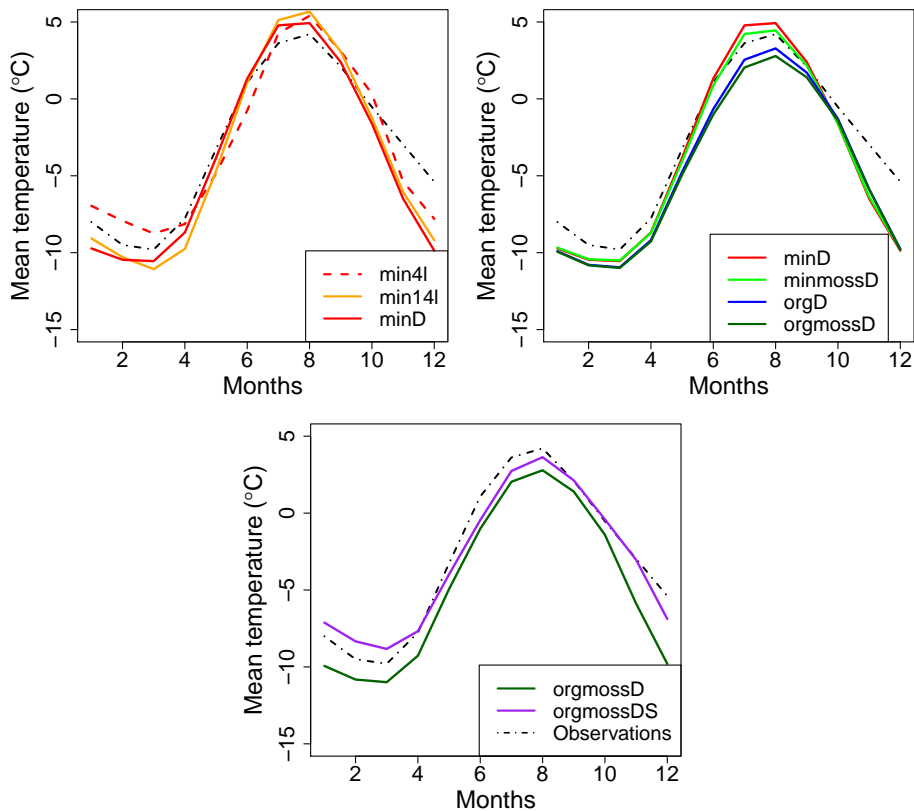


Figure 5. Comparison of annual cycle of soil temperatures at 90 cm depth, from the Russian historical soil temperature and IPY-TSP data (Sect. 2.4.4) and JULES simulations.

Impact of model developments on permafrost simulation in JULES

S. E. Chadburn et al.

Title Page

Abstract Introduction

Conclusions References

Tables Figures

◀ ▶

◀ ▶

Back Close

Full Screen / Esc

Printer-friendly Version

Interactive Discussion



Impact of model developments on permafrost simulation in JULES

S. E. Chadburn et al.

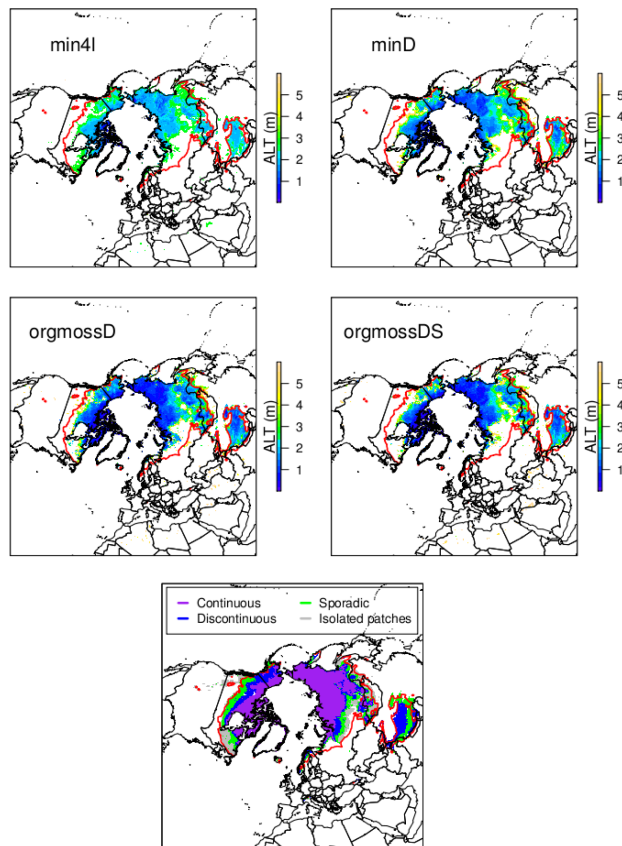


Figure 6. First two rows: Mean active layer thickness in JULES simulations, 1979–1989. Shows all grid cells with active layer ≤ 6 m, with mean ALT indicated by colour. Bottom: Observed permafrost map (Brown et al., 1998), based on maps made between approximately 1960 and 1990. On all plots the zero-degree air temperature isotherm is shown in red (1979–1989 from WFDEI air temperature, see Sect. 2.4.1).

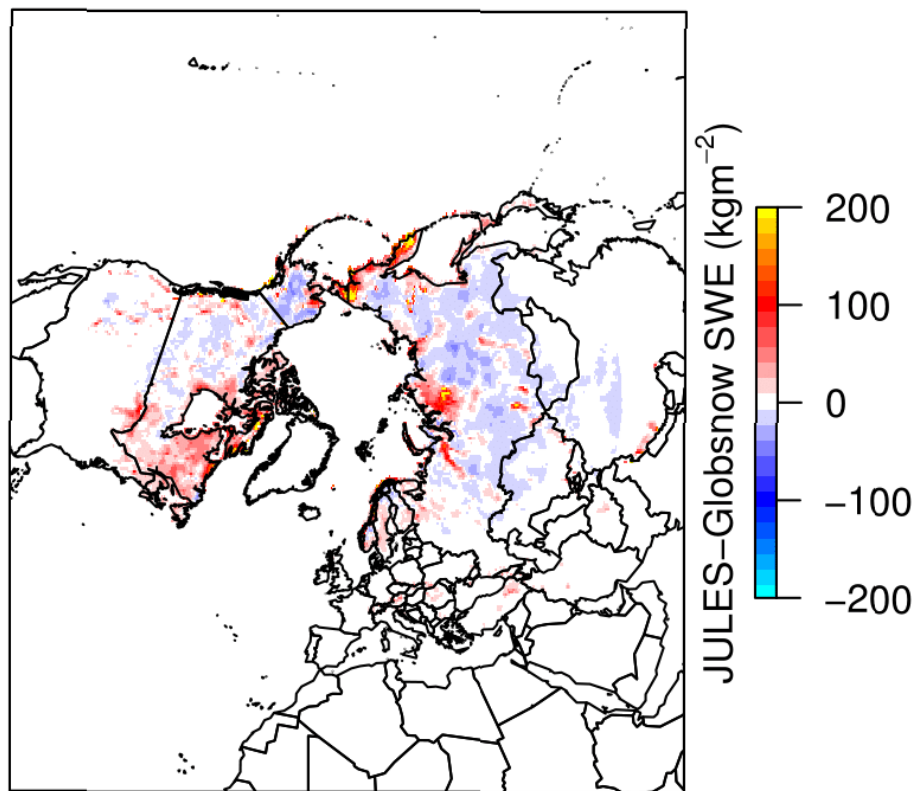


Figure 7. Comparison of Globsnow and JULES. Mean snow water equivalent (SWE) in Globsnow was subtracted from the JULES values over the same time periods. See Sect. 2.4.5.

Impact of model developments on permafrost simulation in JULES

S. E. Chadburn et al.

Title Page	
Abstract	Introduction
Conclusions	References
Tables	Figures
◀	▶
◀	▶
Back	Close
Full Screen / Esc	
Printer-friendly Version	
Interactive Discussion	



Impact of model developments on permafrost simulation in JULES

S. E. Chadburn et al.

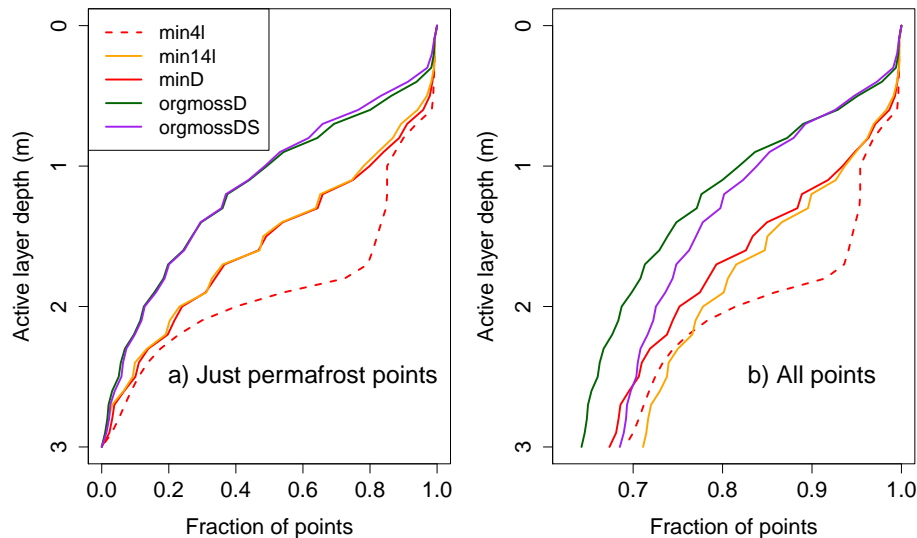


Figure 8. The vertical distribution of permafrost, shown by the fraction of points for which the soil thaws below a given depth. **(a)** Permafrost points only: this includes only those points with ALT less than 3 m, hence 0% of them thaw to below 3 m. **(b)** All points included, hence about 70% thaw to 3 m or deeper. We have one point for each grid cell for each year of the historical simulation.

Title Page

Abstract

Introduction

Conclusions

References

Tables

Figures

◀

▶

◀

▶

Back

Close

Full Screen / Esc

Printer-friendly Version

Interactive Discussion



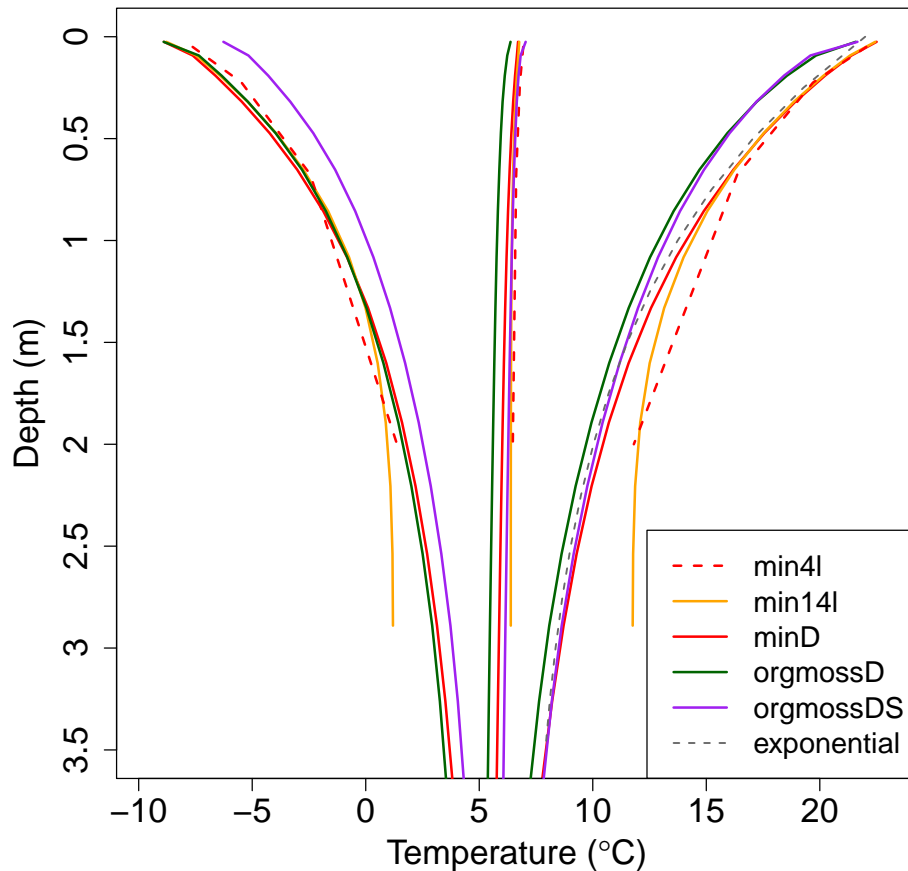


Figure 9. The annual maximum, minimum and mean of simulated soil temperatures (right-hand, left-hand and centre lines respectively), averaged over the period 1979–1989, for the land area north of 50° latitude. Comparing the simulations with different soil depth is of particular interest here.

Title Page

Abstract Introduction

Conclusions References

Tables Figures

◀ ▶

◀ ▶

Back Close

Full Screen / Esc

Printer-friendly Version

Interactive Discussion



Impact of model developments on permafrost simulation in JULES

S. E. Chadburn et al.

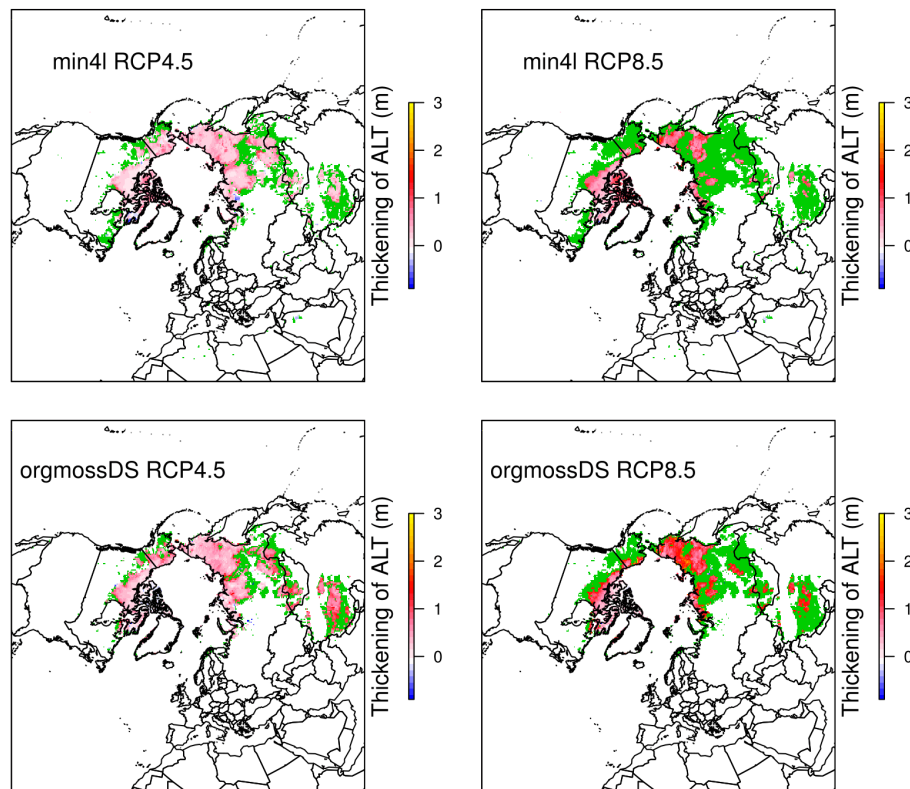


Figure 11. Coloured area shows near-surface permafrost at the start of the simulation: green regions have disappeared by the end of the simulation (2090–2100) and other colours (reddish) show active layer deepening in the remaining permafrost.

[Title Page](#)[Abstract](#)[Introduction](#)[Conclusions](#)[References](#)[Tables](#)[Figures](#)[◀](#)[▶](#)[◀](#)[▶](#)[Back](#)[Close](#)[Full Screen / Esc](#)[Printer-friendly Version](#)[Interactive Discussion](#)